ISSN 1063-7826, Semiconductors, 2010, Vol. 44, No. 8, pp. 1074–1079. © Pleiades Publishing, Ltd., 2010.
Original Russian Text © A.D. Remenyuk, T.K. Zvonareva, I.T. Serenkov, V.I. Sakharov, T.S. Perova, J. Wasyluk, 2010, published in Fizika i Tekhnika Poluprovodnikov, 2010, Vol. 44, No. 8, pp. 1108–1113.

AMORPHOUS, VITREOUS, POROUS, ORGANIC, AND MICROCRYSTALLINE SEMICONDUCTORS; SEMICONDUCTOR COMPOSITES

A Study of Raman and Rutherford Backscattering Spectra of Amorphous Carbon Films Modified with Platinum

A. D. Remenyuk[a]^, T. K. Zvonareva[a], I. T. Serenkov[a], V. I. Sakharov[a], T. S. Perova[b], and J. Wasyluk[b]

[a] *Ioffe Physical Technical Institute, Russian Academy of Sciences, St. Petersburg, 194021 Russia*

^*e-mail: arem@mail.ioffe.ru*

[b] *Department of Electronic and Electrical Engineering, Trinity College, Dublin 2, Ireland*

Submitted January 27, 2010; accepted for publication February 12, 2010

Abstract—Raman spectra have been measured in the spectral range from 1000 to 1800 cm^{-1} on samples of amorphous carbon modified with platinum in amounts comparable with that of carbon. Also, Rutherford backscattering spectra have been studied. It is shown that, as the platinum concentration is raised to ~0.5×10^{22} at cm^{-3}, the average size of graphene clusters increases. As the platinum concentration increases further, the graphene clusters become smaller in size.

DOI: 10.1134/S106378261008021X

1. INTRODUCTION

Amorphous carbon (α-C) has long attracted researchers' attention as a multipurpose material for various coatings. Recently, steadily increasing interest has been aroused by its use as a host for metal–carbon composites. In different times, the role of metal additive has been played by gold [1], titanium [2, 3], chromium [4], iron [5], cobalt [6], copper [7], and a number of other metals. All these metals modify the amorphous carbon matrix and thereby create metallic clusters, rather than becoming a substitution impurity. The properties of these nanoclusters and their effect on the manner in which the amorphous carbon matrix is modified depend on the nature of the modifying metal. Platinum is of particular interest as a modifier because of its being a known catalyst for numerous chemical processes [8]. The carbon film can serve as a support for such a nanocatalyst. Another important specific feature of platinum is its full chemical neutrality toward the material of the carbon matrix.

In our previous study [9], we examined an admixture-free amorphous carbon and α-C modified with platinum by means of ellipsometry, IR absorption spectroscopy, and Raman spectroscopy. It was demonstrated that platinum clusters are incorporated into the system of graphene planes of amorphous carbon. As also in the case of modification of amorphous carbon with cobalt and copper [10, 11], modification with platinum changes the size of chainlike and ringlike graphite structures. Estimating calculations of the size of graphene clusters for unmodified amorphous carbon and that containing platinum in amounts comparable with the content of carbon [9] demonstrate that, with the amounts of platinum we introduced, the structure of the carbon matrix changes only slightly.

The goal of this study was to subject layers of amorphous carbon modified with platinum (α-C–Pt) by magnetron co-sputtering of carbon and platinum to a joint analysis by Raman spectroscopy and Rutherford backscattering of protons. This communication continues a series of articles concerned with the interaction of metallic inclusions with the amorphous carbon matrix [9–12].

2. EXPERIMENTAL

2.1. Sample Fabrication Technique

Amorphous carbon α-C layers had the form of thin films transparent in the visible spectral range. The films were deposited by dc magnetron sputtering of a graphite target in the atmosphere of argon onto single-crystal silicon substrates. This was done using an O1NI-7-006 Oratoriya 5 industrial installation. The sample fabrication procedure was described in more detail in [13].

To introduce platinum into amorphous carbon, i.e., to produce an α-C–Pt composite, we used cosputtering of graphite and platinum also onto Si (111) substrates. The amount of platinum introduced into carbon films was varied by changing the area of the platinum target. The sputtering duration also affects the platinum content of the films because of the different sputtering rates of carbon and platinum [14]. The film thickness was measured with an MII-4 interference microscope. The results of these measurements are listed in Table 1. They are close to those calculated in [15], where results of ellipsometric

measurements of the thickness of thin samples were reported.

2.2. Determination of the Platinum Content of α-C–Pt

The content of platinum was determined by the medium energy ion scattering (MEIS) method, which is a variety of the widely known Rutherford backscattering technique. In the experiment, we measured energy spectra of H^+ ions with an initial energy of 242 keV scattered to an angle of 120°. The spectra were measured in an unoriented ("random") mode, with the direction of the primary beam of H^+ ions constituting an angle of 7° with the (111) direction of the single-crystal silicon of the substrate. In some cases, mostly for films with a small amount of platinum, spectra were also measured in the oriented (channeled) mode, in which the direction of the primary H^+ beam coincided with the (111) direction of the substrate. In this case, the suppression of the flux of ions scattered by the substrate makes it possible to more precisely distinguish the signals determined by the scattering of H^+ ions at "light" atoms of the film: C, N, and O. According to estimation, the fraction of carbon matrix atoms displaced from the equilibrium position upon collisions with protons having the energy used in the experiment is less than 0.3%. Information about the composition of a film was obtained by fitting a film model, including its composition and thickness to the experimental spectrum (MEIS) [16].

2.3. Analysis of Raman Spectra

Raman spectra of α-C–Pt samples were measured at room temperature in the backscattering configuration with a RENISHAW 1000 micro-Raman system equipped with a CCD detector and a Leica microscope. All the measurements were performed using a grating with 1800 lines per millimeter, which provided a spectral resolution of ~1 cm^{-1}. A He–Ne laser (633 nm, 10 mW) served as the excitation source. The measurements were carried out over 30 s with five accumulations in the frequency range 450–1900 cm^{-1}. The laser beam was focused onto the sample surface with a 50 × short-focal-length lens.

3. EXPERIMENTAL RESULTS

3.1. Rutherford Backscattering

Figure 1 shows an energy spectrum of backscattered H^+ ions, measured for sample *3* with a spherical electrostatic energy analyzer (ESA) having a high energy resolution and, accordingly, good depth resolution. Under the conditions used (H^+ ions, initial energy 242 keV, scattering angle 120°), the depth resolution for surface layers of the film is ~2 nm.

Information on the parameters of the film was obtained by comparing its experimentally measured spectrum with that produced by simulation (circles and solid curve in Fig. 1, respectively). The part of the spectrum in the energy range 240–210 keV corresponds to H^+ ions scattered by platinum atoms, and that with energies of 200 keV and lower, to the silicon substrate. In the range 200–170 keV, the signal from the light components of the film, C, N, and O, is superimposed on the signal from the substrate.

Table 1. Parameters of the samples under study

Sample no.	Thickness, nm	Volume concentration of platinum, 10^{22} at cm^{-3}
1	40	0
2	130	1.09
3	90	0.47
4	110	0.97
5	60	1.2
6	70	2.06
7	20	2.0

The amount of platinum found in the simulation was 4.2×10^{16} at cm^{-2}; that of carbon, 2.5×10^{17} at cm^{-2}; and the total amount of nitrogen and oxygen atoms, 1.7×10^{17} at cm^{-2}. The amount of platinum is determined with the highest accuracy (error not exceeding 5%). The error in determining the amount of carbon atoms is substantially larger: 30% according to our estimate. The "flat top" of the Pt peak points to a constant concentration of platinum across the film thickness.

Using data on the geometric thickness of a film as the distance between the film and substrate surfaces,

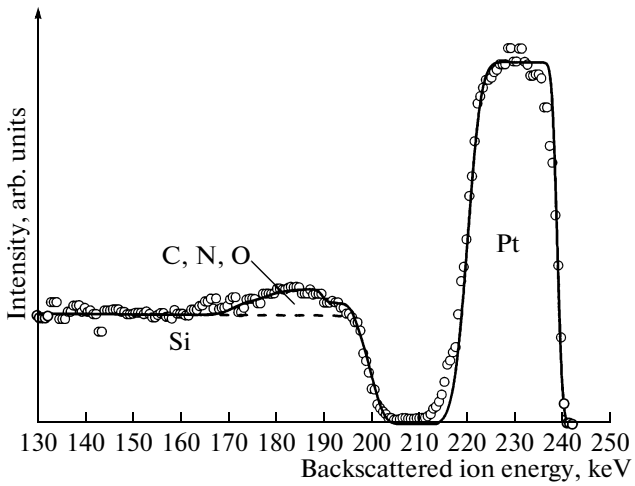

Fig. 1. Experimental (circles) and simulated (solid curve) spectra of H^+ ions with an initial energy of 242 keV scattered to an angle of 120° from sample *3*.

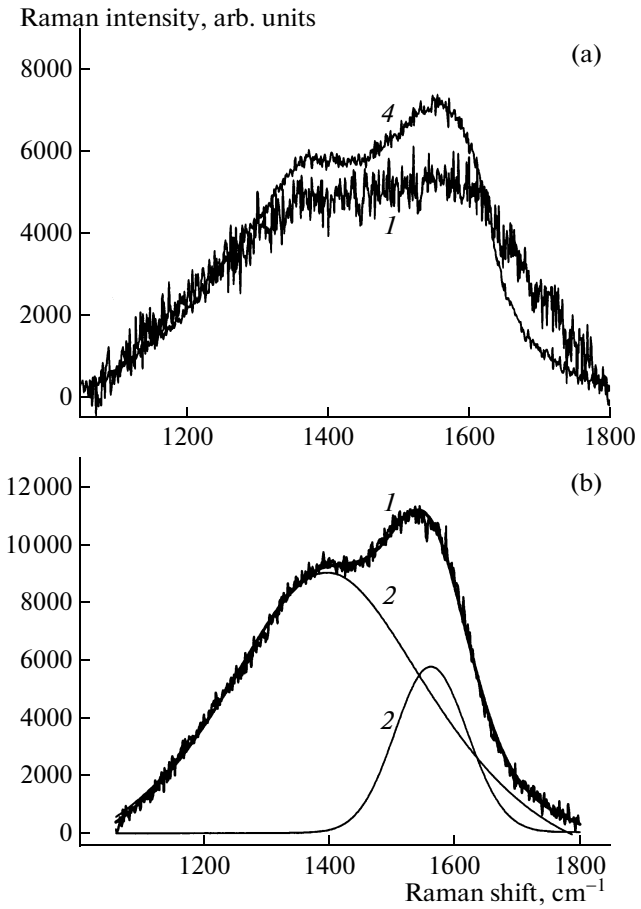

Fig. 2. (a) Raman spectra of platinum-free sample *1* and sample *4* with a platinum concentration of 0.97×10^{22} at cm^{-3}. (b) Raman spectrum of sample *3* with a platinum concentration of 0.47×10^{22} at cm^{-3}. (*1*) Experiment and (*2*) Gaussian approximations.

found by interference measurements, we can determine the volume concentration of platinum atoms in the film. Table 1 lists platinum concentrations in the films studied, according to MEIS data.

Some of the samples contain, in addition to platinum, also hydrogen, oxygen, and nitrogen. Presumably, these elements were introduced into the films in the course of magnetron sputtering via ionization of residual gas molecules in the vacuum chamber.

3.2. Raman Scattering

Figure 2a shows Raman spectra of amorphous carbon for sample *1*, which contains no platinum, and sample *4*, modified with platinum. Figure 2b shows an experimental spectrum and its decomposition into two constituent bands by using a mixture of Gaussian and Lorentzian functions for the platinum-containing sample *3*. The spectra are typical of α-C [11, 7] and contain two known bands: *G* band (graphitic) peaked at 1560–1600 cm^{-1}, and *D* band (disordered) peaked at 1350–1420 cm^{-1}, which are related to sp^2 carbon bonds. In the platinum-free sample, the *D* band is noticeably weaker than the *G* band and only makes the spectrum asymmetric, being a shoulder of the *G* band. The *G* band is due to stretching vibrations of the sp^2 bonds in carbon rings and chains, and the *D* band is associated with breathing modes in carbon rings [11, 18, 19]. The *D* band is due to violation of the selection rules for the wave vector in phonon transitions in the case of small graphene crystallites in the presence of some structure-disturbing factors, e.g., foreign inclusions.

Table 2 lists peak frequencies and full widths at half-maximum (FWHM) for the *D* and *G* bands and the ratio of the peak band intensities. The peak positions of the bands were found by fitting a combination of Gaussian and Lorentzian functions to an experimental Raman spectrum. It can be seen from Table 2 and Fig. 3 that the peak frequency of the *D* band increases with concentration at low platinum concentrations and weakly depends on the platinum content as it increases further within the entire range under study. The peak frequency of the *G* band weakly decreases as the content of platinum grows (Fig. 3), in contrast to the results of [11] for copper and cobalt. The FWHM of the *D* and *G* bands also somewhat decreases with increasing platinum content (Fig. 4),

Table 2. Platinum concentration *N*, peak positions of *D* and *G* (Ω_D and Ω_G), FWHM of *D* and *G* bands (W_D and W_G), intensity ratio of *D* and *G* bands (I_D/I_G), and average size of graphene clusters (L_a) for the samples under study

Sample no.	N, 10^{22} at cm^{-3}	Ω_D, cm^{-1}	W_D, cm^{-1}	Ω_G, cm^{-1}	W_G, cm^{-1}	I_D/I_G	L_a, Å
1	0	1350	425	1605	319	0.98	13.3
2	1.09	1412.5	350	1574.4	124	1.47	16.3
3	0.47	1402	387	1564	133	1.84	18.2
4	0.97	1400	349	1572	128	1.46	16.2
5	1.2	1416	346	1568	136	1.63	17.2
6	2.06	1420	302	1588	151	1.37	15.8
7	2.0	1399	277	1574	159	1.14	14.3

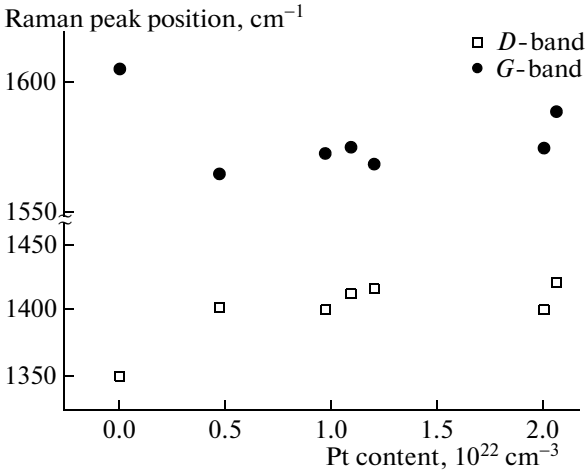

Fig. 3. Peak positions of *D* and *G* bands vs. the platinum content of a film.

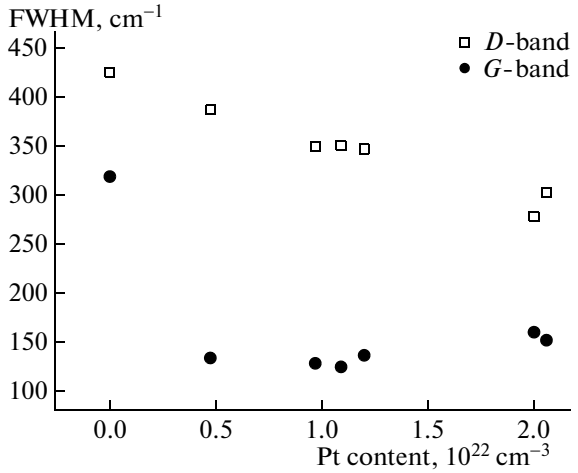

Fig. 4. FWHM of *D* and *G* bands vs. the platinum content of an amorphous carbon film.

which points to a higher degree of graphitization of the Pt-containing films, compared with those composed of pure α-C [20]. The weak dependence of the peak positions of the *D* and *G* bands on the platinum content confirms the opinion that platinum does not give rise to new chemical bonds in the amorphous carbon matrix and weakly affects its structure, with only a charge redistribution caused in graphene clusters, similarly to the case of copper and other metals [3, 5, 6, 10, 21].

The intensity ratio of the *D* and *G* bands, I_D/I_G, shows a nonmonotonic dependence on the platinum content. At low platinum concentrations, I_D/I_G sharply increases, compared with samples containing no platinum and, as the platinum concentration increases further, varies only slightly (Fig. 5). It may be that, at Pt concentrations corresponding to the maximum in Fig. 5, the nature of interaction between platinum atoms and graphene clusters changes and platinum clusters start to be formed in the graphene matrix.

Table 2 also lists sizes of graphene clusters calculated in accordance with [9, 17, 25]. On the assumption that graphene clusters have small sizes, we have

$$I_D/I_G = \gamma L_a^2. \quad (1)$$

Here, L_a is the cluster size and $\gamma = 5.5 \times 10^{-3}$ Å^2 at the excitation wavelength of 515.5 nm, the value obtained by matching at 20 Å formula (1) with the empirical formula

$$I_D/I_G = 44/L_a \quad [22], \quad (2)$$

which is valid when passing from nanographites to a disordered system.

It should be noted that, as can be seen in Figs. 3–5, a wide scatter of points is observed in the dependences of the I_D/I_G ratio, band peak frequency, and FWHM of the bands on the platinum content of a sample. Because the precision of Raman and Rutherford backscattering measurements is fairly high and the values obtained are rather well reproduced in repeated measurements, this scatter is not accidental and reflects the diversity of sample properties, despite the measures taken to well reproduce the film deposition conditions. In particular, a specific property of α-C is the ambivalence allowing simultaneous existence of phases with sp^3, sp^2, and sp^1 hybridizations, which correspond to the following crystalline allotropic modifications: diamond, graphite, and carbine. Therefore, minor differences between samples may consist in differences not only in the platinum content, but also in relative amounts of sp^3, sp^2, and sp^1 bonds. In addition, the results of previous IR

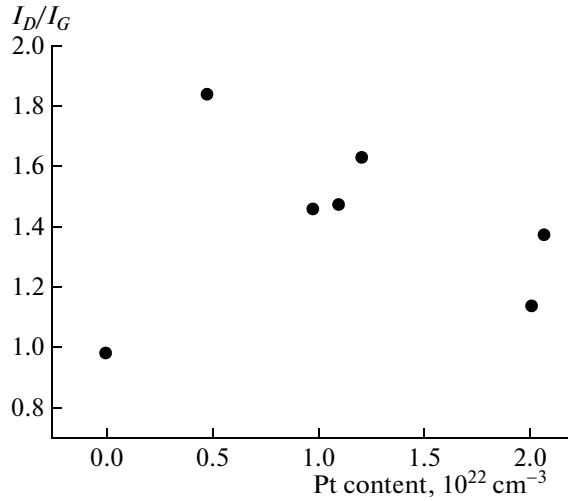

Fig. 5. I_D/I_G ratio vs. the platinum content in the film.

absorption studies [9] demonstrate that spectra of amorphous carbon films contain bands associated with C–O, C=O, O–H, C–H, and, possibly, single, double, and triple C–N bonds. According to Rutherford backscattering data, the films under study also contain nitrogen inclusions. It has been reported previously [19] that presence of nitrogen in an amorphous carbon film hardly affects the Raman spectrum, but gives rise to new active absorption bands in the same spectral range. However, subsequent studies demonstrated [23] that presence of nitrogen rather strongly affects the Raman spectrum of amorphous carbon and the I_D/I_G ratio varies with the platinum content in the same direction as does the dependence of this quantity on the Pt content. Therefore, the I_D/I_G ratio contains for some samples, especially for samples *1* and *3*, a contribution associated with the presence of nitrogen and may be somewhat overstated. Samples *1* and *7* also contain hydrogen, which leads, according to [21, 24], to an increase in the fraction of sp^2 bonds in the structure of the amorphous carbon film. However, the general tendency of variation of the I_D/I_G ratio, FWHM, and peak frequencies of the *D* and *G* bands with the platinum concentration is not affected by these differences.

The question of how the simultaneous presence of various metallic and other incorporated elements affects the Raman spectrum of amorphous carbon requires further, more detailed analysis.

4. CONCLUSIONS

Raman spectra of films of amorphous carbon modified with platinum in amounts from zero to that comparable with the carbon content were studied. The platinum content of the films was determined by the Rutherford backscattering method. It was found that the I_D/I_G ratio grows with increasing Pt/C at small platinum concentrations and the full width at half-maximum of the *G* band decreases. Thus, it was demonstrated that, as the platinum concentration increases to $\sim 0.5 \times 10^{22}$ cm^{-3}, graphene clusters grow in size. As the platinum concentration is raised further, their size decreases. A comparison of the Raman spectra for platinum-free and platinum-containing samples confirmed that the presence of platinum in the amorphous carbon matrix leads to an increase in the fraction of the sp^2 phase in the matrix, in agreement with the results of [21, 24].

ACKNOWLEDGMENTS

We are grateful to V.I. Ivanov-Omskii for helpful discussions.

This study was supported by the programs of the Presidium of the Russian Academy of Sciences "Effect of Atomic-Crystalline Structure on Properties of Condensed Media" (grant 2.15) and "Quantum Physics of Condensed Media" (program P03), the Russian Foundation for Basic Research (projects nos. 09-02-00782 and 08-02-01408), and the Irish Research Council for Science, Engineering & Technology, Ireland.

REFERENCES

1. E. Thune, E. Carpene, K. Sauthoff, M. Seibt, and P. Reinke, J. Appl. Phys. **98**, 034304 (2005).
2. B. Shi, W. J. Meng, and T. L. Daulton, Appl. Phys. Lett. **85**, 4352 (2004).
3. P. Wang, X. Wang, Y. Chen, G. Zhang, W. Liu, and J. Zhang, Appl. Surf. Sci. **253**, 3722 (2007).
4. X. Fan, E. C. Dickey, S. J. Pennicook, and M. K. Sunkara, Appl. Phys. Lett. **75**, 2740 (1999).
5. S. G. Yastrebov, V. I. Ivanov-Omskii, V. A. Kosobukin, F. Dumitrache, and K. Moroshanu, Pis'ma Zh. Tekh. Fiz. **30** (23), 47 (2004) [Tech. Phys. Lett. **30**, 995 (2004)].
6. É. A. Smorgonskaya, T. K. Zvonareva, E. I. Ivanova, I. I. Novak, and V. I. Ivanov-Omskii, Fiz. Tverd. Tela **45**, 1579 (2003) [Phys. Solid State **45**, 1658 (2003)].
7. V. I. Ivanov-Omskii, T. K. Zvonareva, and G. S. Frolova, Fiz. Tekh. Poluprovodn. **34**, 1450 (2000) [Semiconductors **34**, 1391 (2000)].
8. Yu. V. Pleskov, Yu. E. Evstigneeva, and A. M. Baranov, Élektrokhimiya **37**, 755 (2001) [Russ. J. Electrochem. **37**, 644 (2001)].
9. A. D. Remenyuk, T. K. Zvonareva, I. B. Zakharova, V. A. Tolmachev, L. V. Belyakov, and T. S. Perova, Fiz. Tekh. Poluprovodn. **43**, 947 (2009) [Semiconductors **43**, 915 (2009)].
10. V. I. Ivanov-Omskii and É. A. Smorgonskaya, Fiz. Tekh. Poluprovodn. **32**, 931 (1998) [Semiconductors **32**, 831 (1998)].
11. V. I. Ivanov-Omskii and É. A. Smorgonskaya, Fiz. Tekh. Poluprovodn. **39**, 970 (2005) [Semiconductors **39**, 934 (2005)].
12. T. K. Zvonareva, V. I. Ivanov-Omskii, A. V. Nashchekin, and L. V. Sharonova, Fiz. Tekh. Poluprovodn. **34**, 96 (2000) [Semiconductors **34**, 98 (2000)].
13. A. A. Nechitailov, T. K. Zvonareva, A. D. Remenyuk, V. A. Tolmachev, D. N. Goryachev, O. S. El'tsina, L. V. Belyakov, and O. M. Sreseli, Fiz. Tekh. Poluprovodn. **42**, 1273 (2008) [Semiconductors **42**, 1249 (2008)].
14. *Sputtering by Particle Bombardment I*, Ed. by R. Behrisch (Springer, Berlin, 1981; Moscow, Mir, 1984).
15. V. Tolmachev, V. Ivanov-Omskii, T. Zvonareva, A. Nechitailov, V. Shvets, T. Perova, and E. Krutkova, in *Proc. of the 14th Intern. Conf. on Solid Films and Surfaces, June 29–July 4, 2008, Trinity College Dublin, Ireland,* poster Tue P51, httpp://www.icsfs.ie/.
16. V. V. Afrosimov, R. N. Il'in, S. F. Karmanenko, A. A. Melkov, V. I. Sakharov, and I. T. Serenkov, Thin Sol. Films **492**, 146 (2005).

17. A. C. Ferrari and J. Robertson, Phys. Rev. B **61**, 14095 (2000).
18. B. Bousher-Fabre, C. Godet, M. Lacerda, S. Charvet, K. Zellama, and D. Ballutaud, J. Appl. Phys. **95**, 3427 (2004).
19. J. N. Kaufman, S. Metin, and D. D. Saperstein, Phys. Rev. **39**, 1353 (1989).
20. V. I. Ivanov-Omskii, T. K. Zvonareva, and G. S. Frolova, Fiz. Tekh. Poluprovodn. **42**, 1131 (2008) [Semiconductors **42**, 1113 (2008)].
21. V. I. Ivanov-Omskii and É. A. Smorgonskaya, Fiz. Tverd. Tela **41**, 868 (1999) [Phys. Solid State **41**, 786 (1999)].
22. F. Tuinstra and J. L. Koenig, J. Chem. Phys. **53**, 1126 (1970).
23. R. McCann, S. S. Roy, P. Papacostantinou, J. A. McLaughin, and S. C. Ray, J. Appl. Phys. **97**, 073522 (2005).
24. J. Budai, Z. Toth, A. Juhasz, G. Szakacs, E. Szilagyi, M. Veres, and M. Koos, J. Appl. Phys. **100**, 043501 (2006).
25. A. C. Ferrari and J. Robertson, Phys. Rev. B **61**, 14095 (2000).

Translated by M. Tagirdzhanov